Chapter 6: Results and Discussion

This chapter discusses how to put the coil coupling system and power electronics circuit for WPTS into practice. It is first described how to assess spiral coil coupling, together with inductive characteristics and magnetic flux density. Then a coil system and power electronics configuration are described. Both systems finally integrated, and various measurements are taken under various loads.

6.1 Results obtained:

Building, developing, and analysing a low-power wireless power transfer system for the storage system of hybrid electric vehicles (HEV) is the goal of this research. This system will be superior to traditional EV charging systems in terms of efficiency, environmental friendliness, convenience, and flexibility. A square and circular topology for the wireless coil design has been devised and simulated in this study. ANSYS Electronics is used to design both coils. The findings of the simulation point to some extremely intriguing electrical characteristics. In all three directions, misalignments between the transmitting and receiving coils have been examined. In this chapter hardware results are presented and discussed in details.

6.2 Hardware prototype results:

Entire hardware prototype has been tested for WPT and results at all the building blocks are taken for analysis.

6.2.1 Control signal:

Control signals are crucial in a Wireless Power Transfer (WPT) system for regulating and handling the power transfer process effectively and securely. These control signals make sure that the desired operational parameters are maintained while transferring power precisely from the transmitter to the receiver. The typical control signal employed in a WPT system is frequency control signal.

The transmitter and receiver are set to the same resonant frequency thanks to the frequency control signal, which also regulates operational frequency of WPT system. The key to increasing power transmission efficiency is frequency tuning. Frequency adjustments depending on load or environmental circumstances are one type of control approach. Here for

this research frequency of 53.1 kHz has been determined analytically. Output waveforms from the controller ATmega32A is given in Figure 6-1. Control signals are having magnitude of 5 volts with rectangular shape and having dead time of 0.2 micro second.

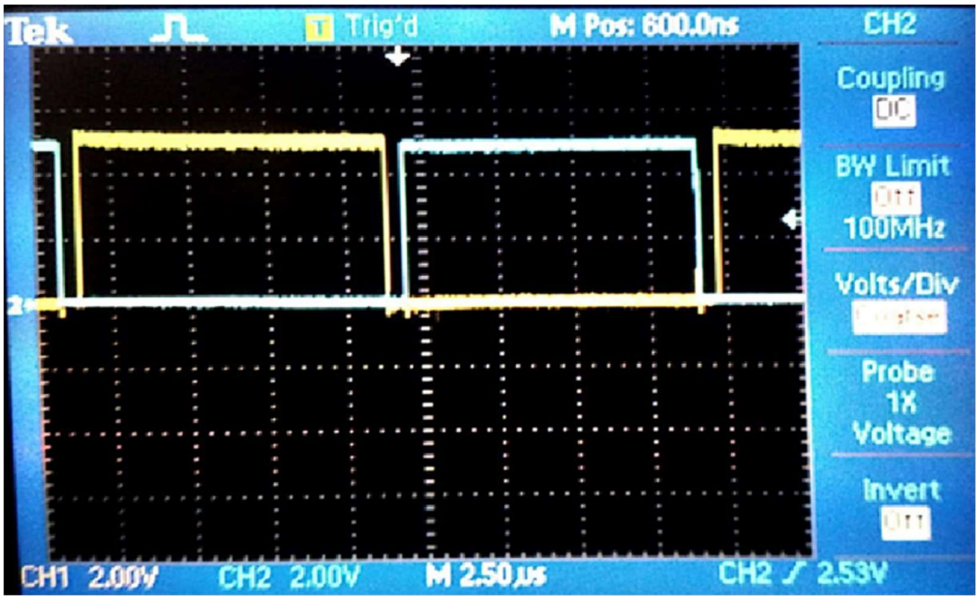

Figure 6-1 Complementary gate signals at microcontroller.

These gate signals are further applied to isolation circuit, which provides electrical isolation between control circuit and power circuit. So, before electrical power circuit (inverter) these gate signals are observed at input and output of isolation circuit. This isolation circuit is made up of opto-couplers. The output waveforms of both input and output of opto-couplers are presented in Figure 6-2 and Figure 6-3.

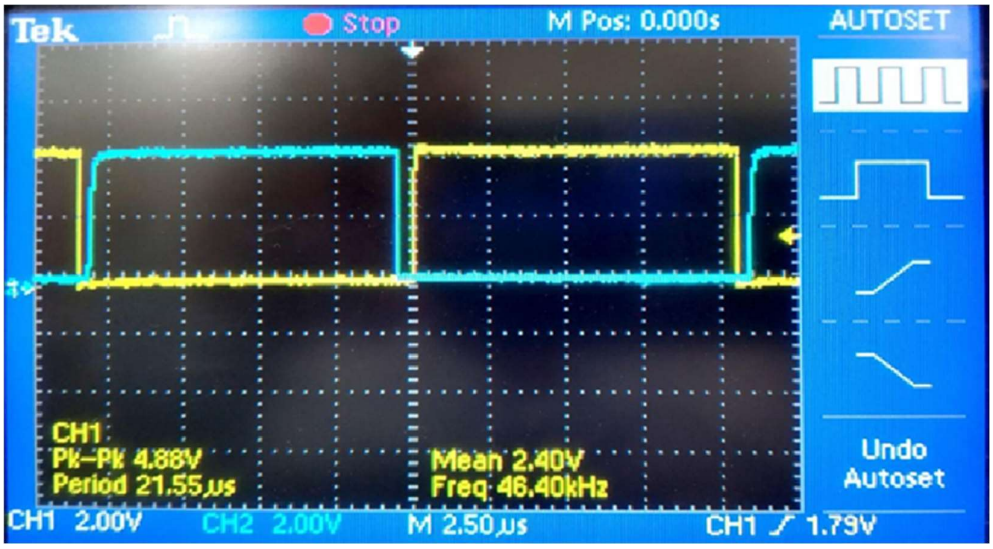

Figure 6-2 Control signal at input terminal of opto-coupler.

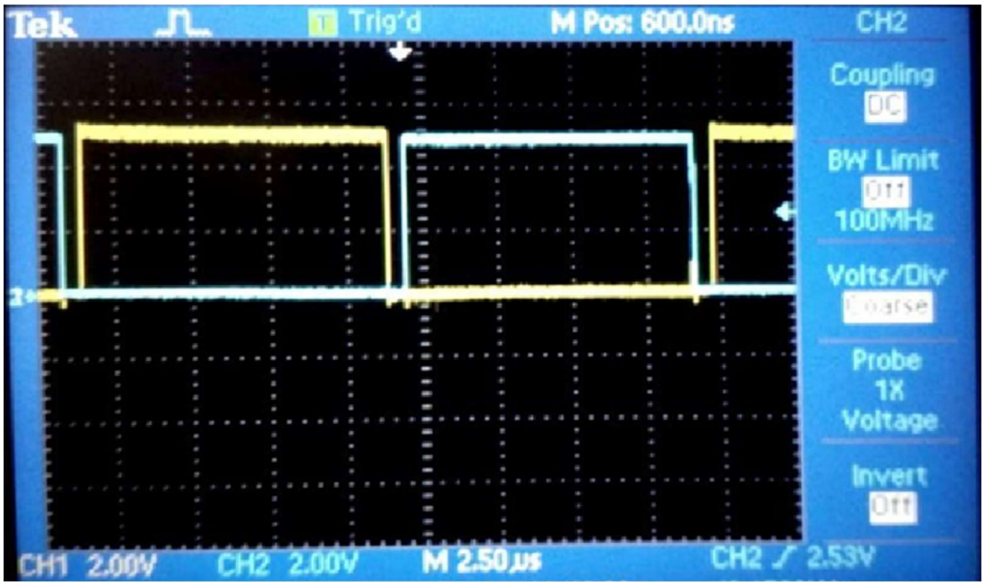

Figure 6-3 Control signal at output terminal of opto-coupler.

Optocoupler circuit and associated connections are given in Appendix-B. We can observe from the waveforms that there is no full similarity between simulation and practical output. These control signals are used for switching the power electronics switches. Here we have used MOSFET as switch to fabricate high frequency inverter. As these MOSFET requires driver circuit for conduction of the power circuit. Figure 6-4 shows output of MOSFET driver circuit output waveform.

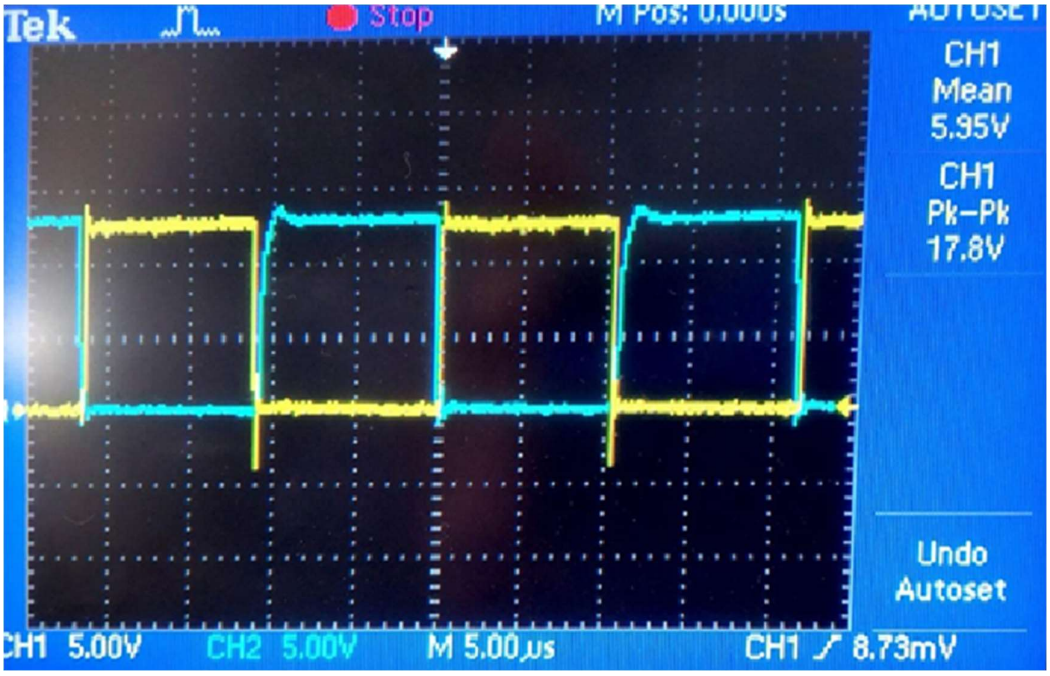

Figure 6-4 Complementary gate pulses at MOSFET driver IRS2110 outputs.

6.2.2 Inverter output:

The output voltage from the inverter is vital in creating the AC (alternating current) signal that is transferred to the transmitter coil in a Wireless Power Transfer (WPT) system. Wireless power transmission is made possible by the magnetic field that an AC signal generates, which is then induced in the receiver coil. A high-frequency AC signal is generally the output voltage of an inverter. The resonance frequency of a WPT system is often taken into account while selecting the frequency, which maximises the efficiency of power transmission. Depending on the system architecture, the waveform may be sinusoidal or another acceptable waveform.

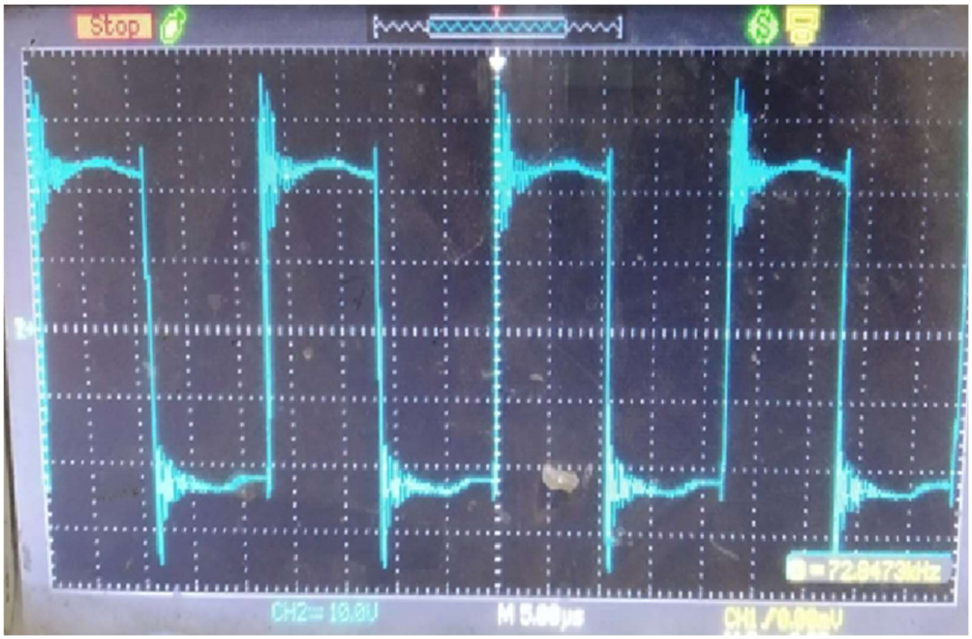

Figure 6-5 Inverter output voltage

Inverter output voltage shown in Figure 6-5 is also supplied to primary side of coupling coil. So, the same voltage waveform is to be consider as input voltage to the primary winding of coil. Output voltage is observed to have transient disturbance, this is due to switching effect.

6.2.3 Coupling coil output:

Coupling coils with square and circular geometry are designed. Both geometries are simulated and results are compared. It was shown that square geometry is most suitable for EV application. So, for experimental verification we have designed square geometry and results are obtained only for same geometry. Figure 6-6 shows output voltage across secondary side of the coil. The output voltage across secondary side of the coil is also having some transients. These transients are as per the input waveform and are due to switching of the power electronics switches (MOSFET in this research).

Figure 6-6 Output voltage across secondary coil.

6.2.4 Output dc voltage:

Finally, the ac voltage across the secondary side of the coil is then fed to rectifier for conversion from ac to dc. This output dc voltage is designed to have 24 volts as an output to charge a battery. Here in this research, a load resister has been connected and output dc voltage represented and shown in Figure 6-7.

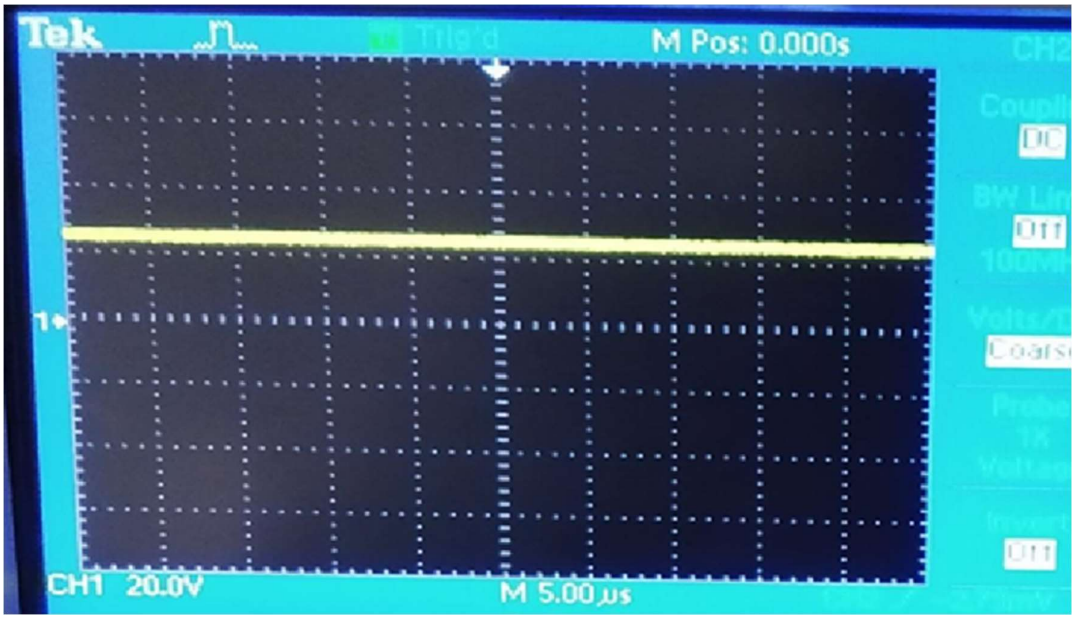

Figure 6-7 Output voltage waveform across load.

Series of experiments have been done on hardware prototype in all the three axis with misalignments. Here for sake of simplicity z-axis and y-axis misalignments are presented in tabular forms and graphical forms.

Ydist/ Zdist	0	25	50	75	100	125	150	175	200
100	76.2	72.4	70.2	66.03	61.31	51.4	41.3	32.3	20.08
75	84.3	82.3	80.01	75.53	71.53	63.4	50.31	36.3	42.4
50	90.1	88.6	83.4	78.38	68.31	65.4	60.13	39.5	37.3
25	95.5	92.2	88.5	82.8	73.54	70.01	61.41	41.3	40
0	98.03	95.12	90.03	80.3	71.03	63.3	53	48	42
-25	95.05	92.2	88.5	82.8	73.54	70.01	61.41	41.3	40
-50	90.01	88.6	83.4	78.38	68.31	65.4	60.13	39.5	37.3
-75	84.3	82.3	80.01	75.53	71.53	63.4	50.31	36.3	42.4
-100	76.3	72.4	70.2	66.03	61.31	51.4	41.3	32.3	20.08

Table 6-1 Experiment results

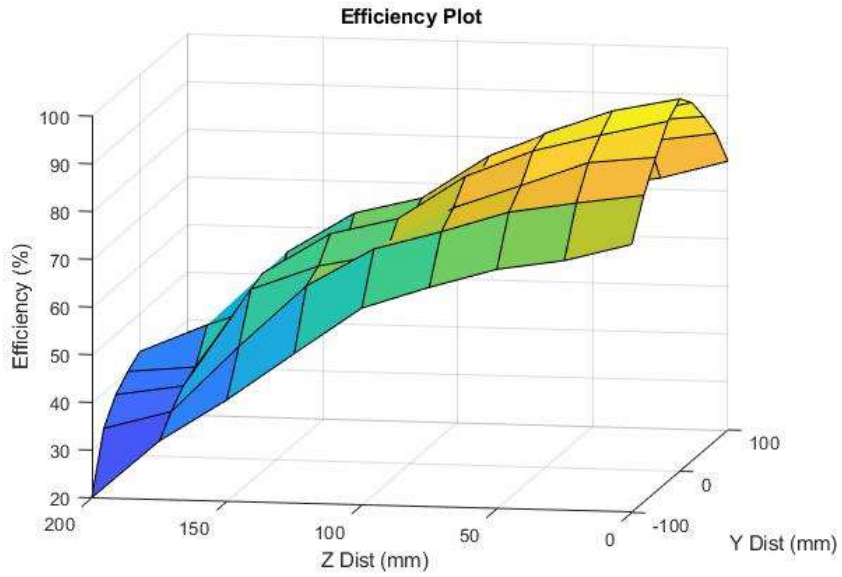

Figure 6-8 Efficiency plot

This chapter demonstrates results obtained from the experiment setup (hardware prototype) to validate the simulation results. It has been observed that a 24 volts dc output voltage is sufficient to charge the battery of 24 volts. The misalignment study has also been carried out for all the 3 directions. Here results are presented for 30 mm vertical misalignment.